

Electrochemical properties and catalytic reactivity of cobalt complexes with redox-active *meso*-substituted porphycene ligands

Taro Koide^a, Zihan Zhou^a, Ning Xu^a, Yoshio Yano^a, Toshikazu Ono^{a,b},
Zhongli Luo^a, Hisashi Shimakoshi^a and Yoshio Hisaeda^{*a,b}

^aDepartment of Chemistry and Biochemistry, Graduate School of Engineering, Kyushu University, Moto-oka 744, Nishi-ku, Fukuoka-shi, Fukuoka 819-0395, Japan

^bCenter for Molecular Systems (CMS), Kyushu University, Moto-oka 744, Nishi-ku, Fukuoka-shi, Fukuoka 819-0395, Japan

Dedicated to Professor Atsuhiko Osuka on the occasion of his 65th birthday.

Received 23 April 2019

Accepted 13 June 2019

ABSTRACT: The cobalt complexes of *meso*-aryl substituted porphycenes were synthesized and characterized. The reduction potentials of the complexes were shifted to the positive side depending on the strength of the electron-withdrawing properties of the *meso*-substituents, while the optical properties, such as the absorption spectra of these complexes, were similar. This suggests that the energy levels of the molecular orbitals of the complexes were changed by the *meso*-substituents while the gaps of the orbitals were not significantly changed. The one-electron reduction of the complex did not afford the Co(I) species, but the ligand-reduced radical anion, which was characterized by electrochemistry. The generated ligand-reduced species reacted with alkyl halides to form the Co(III)-alkyl complex. As a result, the reduction potential of the electrolytic reaction could be directly controlled by the substituents of the porphycene. The catalytic reaction with trichloromethylbenzene was also performed and it was found that the ratio of the obtained products was changed by the reduction potentials of the catalyst, *i.e.* the cobalt porphycenes.

KEYWORDS: cobalt complex, porphycene, ligand reduction, dehalogenation reaction.

INTRODUCTION

Redox-active ligands and/or redox non-innocent ligands for ligand-centered reactions have attracted considerable attention since new reactivity and new reaction mechanisms can be developed by using these ligands [1–3]. While the classic reactions using transition metal complexes were metal-centered, which highly depend on the valence of the central metals, reactions

using metal complexes with redox active ligands depend on the electronic state of both the central metal and the ligand. Collaboration between ligands and central metals offers new types of reactions.

As has been previously reported, the Co(III)-alkyl complex is a key intermediate of the reaction of cobalt complexes and light irradiation leads to homolytic bond cleavage, which affords the Co(II) complex and an alkyl radical [4–9]. Generally, the reactivity of the cobalt complex could be classified by the valence of the cobalt. Lower-valence cobalt has a higher reactivity: for example, in the case of cobalt porphyrin, the Co(I) species generated by one-electron reduction is sufficiently reactive to react with alkyl halides to form Co(III)-alkyl

*Correspondence to: Yoshio Hisaeda, Department of Chemistry and Biochemistry, Graduate School of Engineering, Kyushu University, Moto-oka 744, Nishi-ku, Fukuoka-shi, Fukuoka 819-0395, Japan. tel.: +81-92-802-2826, fax: +81-92-802-2827, email: yhisatcm@mail.cstm.kyushu-u.ac.jp.

complexes [10–15]. However, the Co(II) species is less reactive and cannot react with alkyl halides, but can react with an alkyl radical to afford the Co(III)-alkyl complex [16, 17]. There have been several reports of cobalt complexes using redox-active ligands [3, 18–23].

Recently, we reported the cobalt–carbon bond formation of cobalt porphycene with alkyl halides triggered by the reduction of a ligand [24]. In this reaction system, the electronic state of the ligand, porphycene, changes from an 18π aromatic to an open-shell 19π radical anion due to the low-lying LUMO of the porphycene [24–27]. Of course, the reactivity of the ligand increases, but the reaction occurs at the cobalt center, indicating the activation of the central metal by reduction of the ligand. Using a combination of both experimental and theoretical methods, we revealed the reaction mechanism: the porphycene ligand works as a non-innocent ligand and the cobalt reacts with an alkyl halide *via* the S_N2 -type transition state. This result encouraged us to further investigate the porphycene ligand for application to the catalytic reaction. We also reported the effect of peripheral modification of the ligand. The hydrogenation of the β position of the porphycene caused a change in the reduction site from the ligand to central cobalt to afford the Co(I) species by one-electron reduction [28]. However, the synthesis and peripheral modification of porphycene are rather difficult compared to porphyrin [29, 30]. For a better understanding of the effect of the electronic state of the ligand, systematic tuning of the redox potentials by the introduction of substituents is important.

In this study, for the efficient modification of cobalt porphycene, we selected the *meso*-substituted porphycenes, which can be prepared in shorter steps with a high yield [31–33]. We synthesized several Co(II) complexes with the periphery modified porphycenes and carried out electrochemical experiments and catalytic dehalogenation reactions. Since the one-electron reduction of the ligand promotes the reaction, it could be expected that the modification of the ligand directly affects the reactivity of the complex.

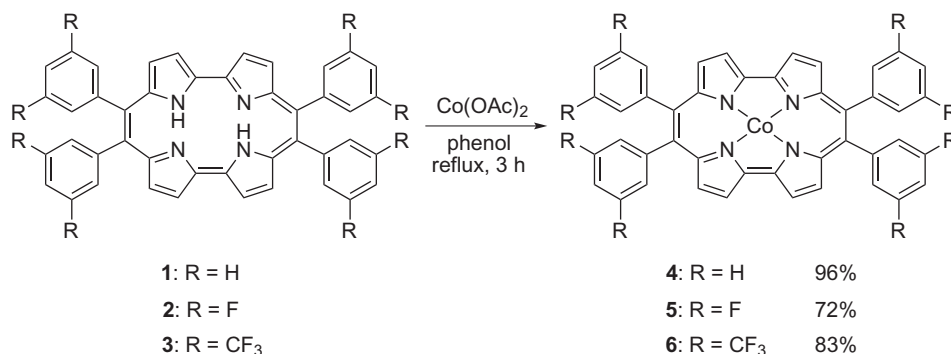
RESULTS AND DISCUSSION

Synthesis and characterization

The *meso*-substituted porphycenes, 9,10,19,20-tetra-phenylporphycene **1**, 9,10,19,20-tetrakis(3,5-difluorophenyl)porphycene **2**, and 9,10,19,20-tetrakis(3,5-bis(trifluoromethyl)phenyl)porphycene **3**, were synthesized by following earlier reported procedures [33]. The cobalt complexes **4**, **5**, and **6** were prepared by the metallation of each porphycene, *i.e.* **1**, **2**, and **3**, with cobalt acetate in phenol under refluxing conditions for 3 h. The yields of the cobalt complexes **4**, **5**, and **6** were 96%, 72%, and 83%, respectively (Scheme 1). The structure of **5** was revealed by a single crystal X-ray diffraction analysis [34]. The cobalt ion was inserted into the central cavity and the porphycene skeleton had a planar structure with a mean plane deviation of 0.016 Å for the twenty carbon and four nitrogen atoms of the porphycene macrocycle. The *meso*-3,5-difluorophenyl substituents were perpendicular to the porphycene plane, indicating that there might be no π -extension effect by the introduction of the *meso*-aryl substituents (Fig. 1). The UV-vis absorption spectra of **4**, **5**, and **6** exhibited similar shapes with the Soret band and Q band at 390 and 625 nm, 390 and 618 nm, and 392 and 619 nm, respectively, indicating that the corresponding band gaps of the MOs of each complex are almost the same (Fig. 2).

Electrochemistry

The electronic effect of the *meso*-substituents was confirmed by electrochemical analysis; *i.e.* cyclic voltammetry (CV). The electrochemical analyses were all performed under nitrogen in a glove box. As expected, both reduction potentials and oxidation potentials were shifted to the positive side in the order of **4** < **5** < **6**. All of them showed two reversible reduction processes. The first reduction potentials of **4**, **5**, and **6** were exhibited at -0.623, -0.525, and -0.454 V (*vs.* Ag/AgCl), respectively, which were shifted depending on



Scheme 1. Synthesis of Co(II) porphycenes with *meso*-aryl substituents

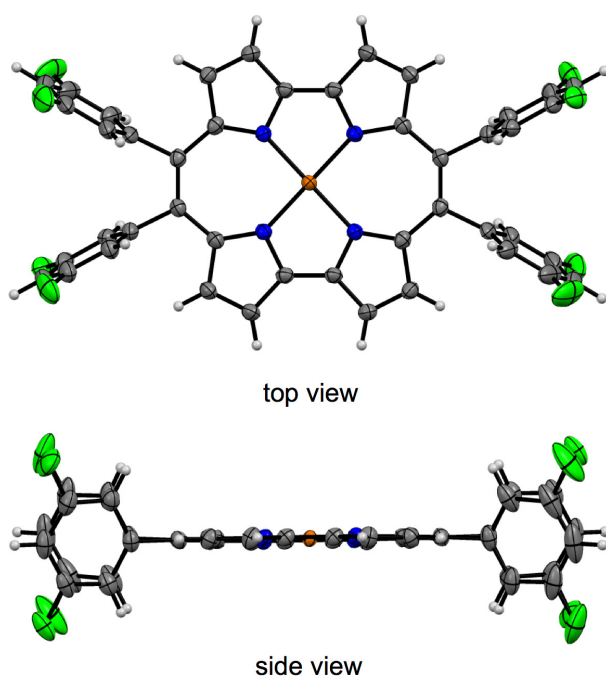


Fig. 1. X-Ray crystal structures of **5**. Thermal ellipsoids are drawn at the 50% probability level. Solvent molecules were omitted for clarity

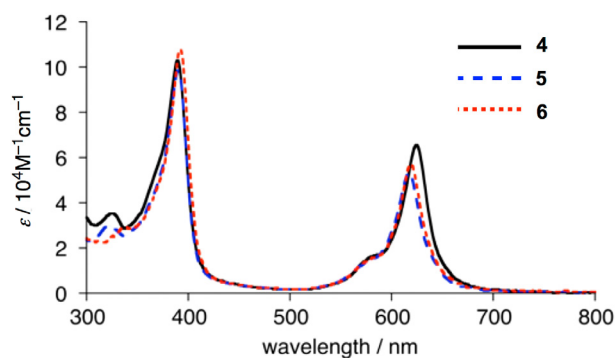


Fig. 2. UV-vis absorption spectra of **4**, **5**, and **6** in CH_2Cl_2

the strength of the electron-withdrawing properties of the substituents (Fig. 3). This result indicates that the *meso*-aryl substituents do not affect to the HOMO–LUMO energy gaps but do affect the energy levels of the molecular orbitals.

Electrospectrochemistry

To confirm the generation of radical anion species of the cobalt porphyrines **4**, **5**, and **6**, the absorption spectra and ESR spectra were measured. In the case of **4** in DMF, the original absorptions at 390 and 635 nm became weaker and new absorption bands at 755 and 880 nm appeared under the reduction potential of -0.80 V (*vs.* Ag/AgCl). The absorption bands at 755 and 880 nm disappeared and a broad absorption between 250–500 nm was observed

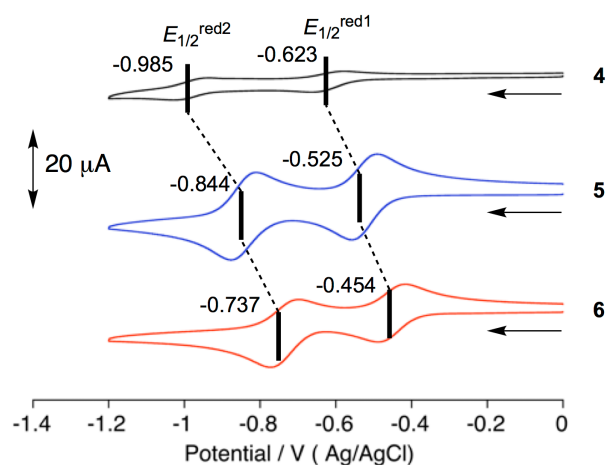


Fig. 3. Cyclic voltammograms of **4**, **5**, and **6** in DMF

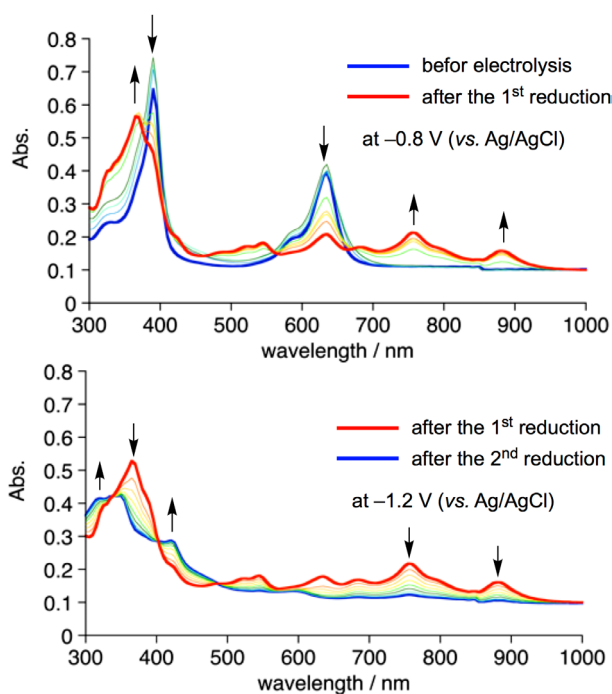


Fig. 4. Time-resolved UV-vis absorption spectra for the reduction of **4** in DMF + 0.1 M TBAClO₄ at a controlled potential of -0.8 and -1.2 V for the 1st and 2nd reduction steps, respectively. WE: Pt mesh, CE: Pt, RE: Ag/AgCl

after the second reduction step at -1.20 V (*vs.* Ag/AgCl) (Fig. 4). Similar spectral changes were observed for **5** and **6** under the reduction potential of -0.70 and -1.1 V and -0.60 and -1.0 V (*vs.* Ag/AgCl), respectively (Figs S1 and S2). The dramatic change in these absorption spectra indicated that the one-electron reduction did not occur at the cobalt center but at the porphyrine ligands to afford the radical anion species by the first reduction step and that the radical anion species disappeared by the second reduction (Scheme 2a) [24–26]. The electron

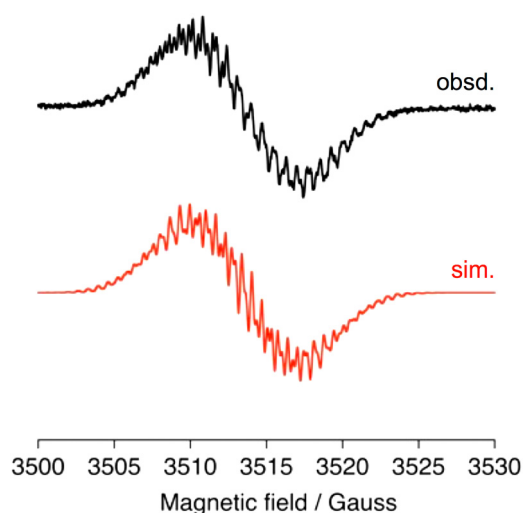


Fig. 5. ESR spectrum of the one-electron reduced species of **4** after the electrolysis at -0.8 V for 1 h and the simulated spectrum

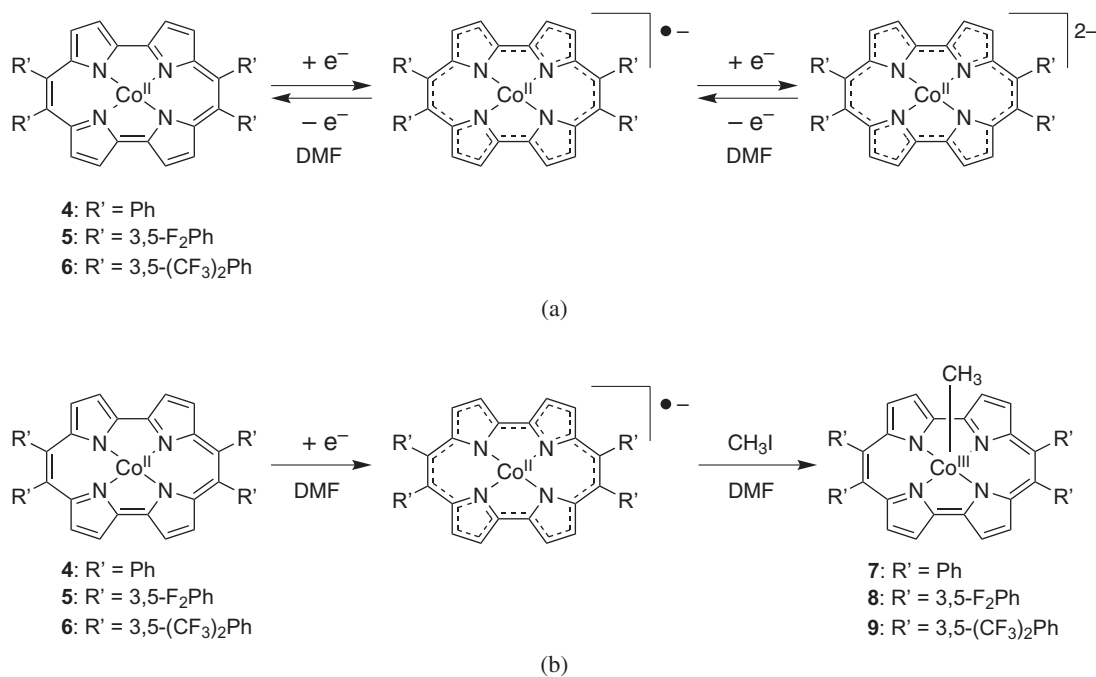
spin resonance (ESR) spectrum of **4** after the electrolysis showed a signal at $g = 2.0071$ with complicated hyperfine couplings, which could be assigned to the organic radical delocalized on the macrocyclic conjugation system of the porphyrine ligand. Based on the simulation of the spectrum, the hyperfine coupling constants (A values) were 0.741 (4H), 0.709 (4H), 0.640 (8H), 0.639 (8H) and 0.600 (4H) G, indicating that the unpaired electron is delocalized not only on the porphyrine skeleton, but also on the phenyl rings at the *meso*-positions (Fig. 5). Although the ESR signal observed for the one-electron reduced species of **5** and **6** did not show an assignable

hyperfine coupling signal, the g values of the signals were 2.0031 and 2.0030 , respectively, suggesting the generation of a ligand-reduced species of the cobalt complexes (Figs S3 and S4).

Reaction with alkyl halide and characterization of cobalt-alkyl complex

Next, the reactivities of the cobalt porphyrines with alkyl halides were explored. After the addition of 50 equivalents of iodomethane to the solution, the cyclic voltammograms of **4**, **5**, and **6** were changed. In the case of **4**, a new reduction wave appeared at -0.735 V, shifted to the negative side compared to the original reduction wave, suggesting the reaction of the one-electron reduced species with iodomethane in the system. The new reduction processes observed at -0.709 and -1.007 V after the addition of iodomethane could be assigned to the reduction potential from the neutral state to the radical anion state and from the radical anion to dianion species of the Co(III)-CH_3 complex (Fig. 6). This phenomenon is the same for the other cobalt complexes, **5** and **6**. The reduction potentials observed by CV in the presence of iodomethane for **5** and **6** were -0.614 , -0.889 V and -0.534 , -0.782 V (*vs.* Ag/AgCl), respectively (Figs S8 and S9). The newly appearing redox waves were also reversible, indicating the stability of the generated Co(III)-CH_3 complexes under the reductive conditions.

The Co(III)-CH_3 complexes **7**, **8**, and **9** were prepared by bulk electrolysis using carbon felt as the working electrode in an undivided cell in DMF with 50 equivalents of iodomethane and purified by filtration after adding water to the reaction mixture to obtain the



Scheme 2. (a) Two step one-electron reduction of **4**, **5**, and **6** and (b) electrolytic synthesis of Co(III)-CH_3 complexes **7**, **8**, and **9**

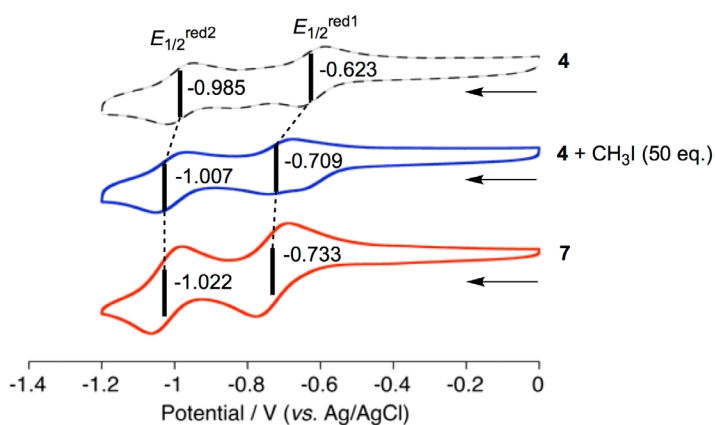


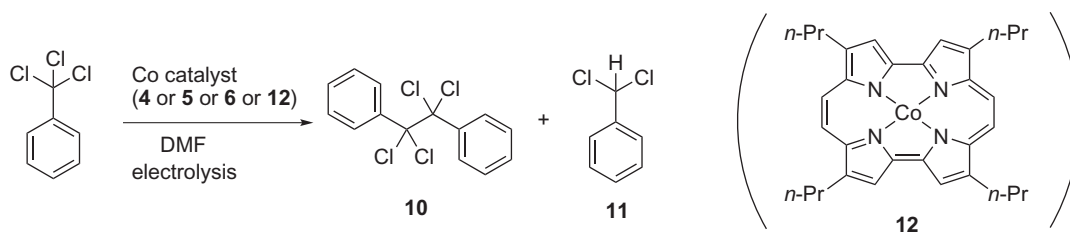
Fig. 6. Comparison of the cyclic voltammograms of **4**, **4** with CH_3I (50 equiv.), and **7** in DMF

product as a precipitate. The obtained solid was washed with methanol/water in the dark (Scheme 2b). From the ^1H NMR spectrum of **7**, the signal of the methyl proton was observed at -4.16 ppm (Fig. S5). The high field shift of the methyl proton indicated the shielding effect by the ring current of the porphycene since the methyl group is located on the central cobalt as the axial ligand. Focusing on the signals of the phenyl groups, signals of *ortho*- and *meta*- protons were exhibited as two signals for each, indicating that the protons of upper side and lower side against the porphycene plane were distinguishable because of the existence of the methyl group as the axial ligand. These features of the ^1H NMR spectrum were similar for those of **8** and **9** (Figs S6 and S7). The reduction potentials of the isolated $\text{Co}-\text{CH}_3$ complex were -0.733 and -1.022 V (vs. Ag/AgCl), which are consistent with the observed reduction potentials of **4** with CH_3I (Fig. 6). The cyclic voltammogram of **8** and **9** also exhibited two reversible reduction processes at -0.604 and -0.870 V and -0.534 and -0.785 V (vs. Ag/AgCl), respectively, which showed good agreement with the results of the CVs of **5** and **6** with iodomethane (Figs S8 and S9). Based on the above results, the reaction mechanism could be proposed in which the one-electron reduced anion radical species of the $\text{Co}(\text{II})$ porphycene reacts with the alkyl halide to form the $\text{Co}(\text{III})$ -alkyl complex. Thus, it could be said that the introduction of *meso*-substituents to the porphycene skeleton effectively

changes the first reduction potential of the cobalt porphycene, which corresponds to the energy level of the LUMO, and the reaction *via* the ligand-reduced species of the cobalt porphycene proceeds under a controlled reduction potential.

Catalytic properties

For further application of this reactivity, we performed a catalytic reaction using trichloromethylbenzene as a substrate, which had been reported for the system using a vitamin B_{12} derivative as a catalyst [35]. The electrolytic reaction of cobalt porphycene with trichloromethylbenzene was first monitored by a CV measurement in DMF. For complex **4**, the catalytic current was observed at around -0.6 V (vs. Ag/AgCl) and the reduction process became irreversible, indicating the formation of the $\text{Co}(\text{III})$ -alkyl complex and the fast cleavage of the cobalt-carbon bond in the system. The bond dissociation gave the alkyl radical, the porphycene cobalt complex returned to the $\text{Co}(\text{II})$ neutral state and the catalytic reaction proceeded. For complexes **5** and **6**, the cyclic voltammograms also showed similar behaviors with the catalytic current at positively shifted potentials compared to that of **4**. For a better understanding of this reaction, bulk electrolysis in an undivided cell using carbon felt as the working electrode, 200 equivalents of trichloromethylbenzene as the substrate, biphenyl as the internal standard was done to analyze the product by GC-MS. The reaction of each cobalt complex, **4**, **5**, and **6**, was carried out at -0.80 V, -0.70 V, and -0.60 V (vs. Ag/AgCl), respectively, for 3 h and the resulting products were analyzed by GC-MS after the purification by short silica gel column chromatography. The electrolysis potentials were selected to be able to generate the one-electron reduced species of each complex. The same reaction was performed using β -tetrapropyl porphycene $\text{Co}(\text{II})$ complex **12** [24] at -1.20 V (vs. Ag/AgCl) for the comparison. From the GC-MS analysis, there were two main products: one was 1,2-diphenyl-1,1,2,2-tetrachloroethane **10** and the other was dichloromethylbenzene **11** (Scheme 3). In the case of complex **4**, **5**, and **6**, the main product was **10** and only a little amount of **11** was observed, while the conversion rate, yield and turnover number (TON) decreased as



Scheme 3. Catalytic dehalogenation and dimerization reaction of trichloromethylbenzene using $\text{Co}(\text{II})$ porphycenes as a catalyst under electrochemical reductive conditions. **12** is the previously reported complex

Table 1. The yields of the products of the catalytic reaction checked by GC-MS analysis

Catalyst	Electrolysis potential/V	Conversion	10	11	TON
4	-0.8	62%	53%	2%	110
5	-0.7	50%	47%	<1%	94
6	-0.6	37%	21%	<1%	42
12	-1.2	28%	15%	12%	54

the electrolysis potential become more positive (Table 1). TON is calculated from the yield of the products against the catalyst, cobalt porphycene. The results were different from that using the complex **12** as a catalyst. When **12** was used as a catalyst, a considerable amount of the simply reduced species (dechlorinated species) **11** was also observed along with the dimer **10**. The generated alkyl radical is more easily reduced at a more negative potential and gave the anion species, which became a dehalogenated product of the substrate **11**, suggesting that the peripheral modification of the porphycene ligand is effective to control the reduction potentials, reactivity, and the products of the catalytic reaction.

EXPERIMENTAL

General

Reagents and solvents of best grade available were purchased from commercial suppliers and were used without further purification unless otherwise noted. Dried dichloromethane (CH_2Cl_2) was obtained by distillation from CaH_2 under a N_2 atmosphere.

Nuclear magnetic resonance (NMR) spectra were recorded on a Bruker Avance 500MHz NMR spectrometer. The resonance frequencies were 500 MHz for ^1H . Chemical shifts were reported as δ values in ppm relative to tetramethylsilane. High-resolution fast atom bombardment mass spectra (HR-FAB-MS) were measured with 3-nitrobenzyl alcohol (NBA) as a matrix and recorded on a JMS-700 spectrometer (JEOL, Japan). Ultraviolet–visible–near infrared (UV-vis-NIR) absorption spectra were recorded on U-3310 spectrometer (Hitachi, Japan) and V-670KS spectrometer (JASCO, Japan). Electron spin resonance (ESR) measurement was carried out with a Bruker EMX 8/2.7. The simulation of the ESR spectrum was carried out using Bruker WinEPR SimFonia software.

Redox potentials were measured by cyclic voltammetry method on an ALS electrochemical analyzer model 630C in a glove box. Cyclic voltammetric measurements were carried out using a 1.6 mm diameter platinum working

electrode and a platinum wire counter electrode in dehydrated solvents containing 0.1 M Bu_4NClO_4 as a supporting electrolyte under a nitrogen atmosphere at room temperature. In the experiment, we employed a Ag/10 mM AgCl reference electrode. The reference electrode was separated from the bulk solution by a fritted-glass bridge filled with 0.1 M NaCl aqueous solution.

Data from X-ray diffraction were collected on a Rigaku XtaLAB mini diffractometer at 123(2)K using Mo $K\alpha$ radiation ($\lambda = 0.71073 \text{ \AA}$). Collected data were integrated, corrected, and scaled using the program CrysAlisPro. The structures were refined using SHELXT (Sheldrick, 2015) Intrinsic Phasing and SHELXL (Sheldrick, 2015). The program Olex2 was used as a graphical interface. All non-hydrogen atoms were refined anisotropically. Hydrogen atoms were located at calculated positions.

The gas chromatography-mass spectra (GC-MS) were obtained using a Shimadzu GCMS-QP 2010 equipped with an Agilent J&W DB-1 column (length:30 m; ID: 0.25 mm, film: 0.25 μm) with helium as the carrier gas. For the measurement, the injector and detector temperatures were 250 $^\circ\text{C}$, the oven temperature was initially held at 100 $^\circ\text{C}$ for 2 min, then increased to 240 $^\circ\text{C}$ at the rate of 10 $^\circ\text{C}/\text{min}$.

Synthesis

Synthesis of freebase porphycenes, 1, 2 and 3. Meso-substituted porphycenes **1**, **2** and **3** were synthesized as described in the literature [33].

Synthesis of meso-tetraphenylporphycene cobalt complex 4: Synthesis of the cobalt complex **4** is described in another paper [34].

Synthesis of meso-tetrakis(3,5-difluorophenyl)porphycene cobalt complex 5. A mixture of tetrakis(3, 5-difluorophenyl)porphycene **2** (10.0 mg, 0.013 mmol), cobalt(II) acetate tetrahydrate (32.0 mg, 0.13 mmol) and phenol (5 mL) were reflux at 170 $^\circ\text{C}$ for 3 h. After cooling to room temperature, the mixture was dissolved using CH_2Cl_2 . The organic layer was washed with water once, with a 5% NaOH solution 10 times and with water again once, then dried over anhydrous Na_2SO_4 and purified by a silica gel column with CH_2Cl_2 . After evaporation the main aquamarine band was collected. The solvent was evaporated to yield **5** as purple solid (7.70 mg, 72%). UV-vis (CH_2Cl_2): λ_{max} , nm ($\epsilon/\text{M}^{-1}\cdot\text{cm}^{-1}$) = 323 (29700), 390 (98500), 617 (53600). HR-MS (FAB): m/z 815.0894 (calcd. for $[\text{M}]^+$ 815.0892). Anal. calc. for: $\text{C}_{44.5}\text{H}_{21}\text{CoN}_4\text{Cl}$ ($\text{C}_{44}\text{H}_{20}\text{CoN}_4 + 0.5 \text{ CH}_2\text{Cl}_2$): C, 62.29; H, 2.47; N, 6.53%. Found: C, 62.26; H, 2.45; N, 6.65.

Synthesis of meso-tetrakis(3,5-bis(trifluoromethyl)phenyl)porphycene cobalt complex 6. A mixture of tetrakis(3, 5-bis(trifluoromethyl)phenyl)porphycene **3** (23.0 mg, 0.0189 mmol), cobalt(II) acetate tetrahydrate (50.0 mg, 0.201 mmol) and phenol (10 mL) were refluxed at 170 $^\circ\text{C}$ for 3 h. After cooling to room temperature, the

mixture was dissolved by CH_2Cl_2 . The organic layer was washed with water once, with 5% NaOH solution 10 times, and with water for once, then dried over anhydrous Na_2SO_4 and purified by silica gel column with CH_2Cl_2 . After evaporation, the main aquamarine band was collected. The solvent was evaporated to yield **6** as purple solid (20.0 mg, 83%). UV-vis (CH_2Cl_2): λ_{max} , nm ($\epsilon/\text{M}^{-1}\cdot\text{cm}^{-1}$) = 299 (21500), 336 (sh, 28500), 392 (108000), 619 (58900). HR-MS (FAB): m/z 1215.0623 ($[\text{M}]^+$ 1215.0637). Anal. calc. for: $\text{C}_{52}\text{H}_{20}\text{CoF}_{24}\text{N}_4$: C, 51.38; H, 1.66; N, 4.61%; Found C, 51.56; H, 1.80; N, 4.56.

Synthesis of porphycene cobalt-methyl complexes 7–9. The controlled-potential electrolysis of porphycene cobalt complex **4–6** (2×10^{-3} mmol) was dissolved in DMF (5 mL) with 0.1 M *n*-Bu₄NClO₄. The solution was carried out in a one-compartment cell with a zinc plate anode as a sacrificial electrode and a carbon felt cathode and electrolysis at -0.8, -0.7, or -0.6V vs. Ag/AgCl in glove box at room temperature. The zinc electrode was used as a sacrificial anode. Electrolysis for one hour and then 50 equiv. CH_3I was added, continue stirring for 5 min under electrolysis conditions. The solution was diluted with water and the solvent was removed by filtration, then the solid was washed with a 50% methanol aqueous solution, and dried under reduced pressure to afford the porphycene cobalt methyl complexes **7–9** as purple solids in about 100% yield.

Compound 7. Electrolysis at -0.8V vs. Ag/AgCl for 1 h. ¹H NMR (500 MHz, CDCl_3): δ_{H} , ppm 9.14 (4H, d, β -H), 8.29 (4H, d, β -H), 7.83 (4H, m, Ph), 7.23–7.35 (16H, m, Ph), -4.16 (3H, s, CH_3). UV-vis (CH_2Cl_2): λ_{max} , nm 291 (sh), 390, 626.

Compound 8. Electrolysis at -0.7V vs. Ag/AgCl for 1 h. ¹H NMR (500 MHz, CDCl_3): δ_{H} , ppm 9.21 (4H, d, β -H), 8.33 (4H, d, β -H), 7.39 (4H, d, Ar), 6.98 (4H, d, Ar), 6.91 (4H, m, Ar), -4.16 (3H, s, CH_3). UV-vis (CH_2Cl_2): λ_{max} , nm 288, 390, 618.

Compound 9. Electrolysis at -0.6V vs. Ag/AgCl for 1 h. ¹H NMR (500 MHz, CDCl_3): δ_{H} , ppm 9.29 (4H, d, β -H), 8.25 (4H, d, β -H), 8.20 (4H, s, Ar), 7.90 (4H, s, Ar), 7.85 (4H, s, Ar), -3.95 (3H, s, CH_3). UV-vis (CH_2Cl_2): λ_{max} , nm 277, 392, 620.

CONCLUSION

The cobalt complexes of the *meso*-aryl substituted porphycenes, **4**, **5**, and **6**, were synthesized and characterized by MS, UV-vis absorption, elemental analysis and X-ray diffraction analysis. Their electrochemical properties were explored by CV and DPV. The reduction potentials of each complex were shifted in the order of **4** < **5** < **6**, depending on the strength of the electron-withdrawing effect of the *meso*-substituents. The one-electron reduction of these Co(II) porphycenes produced the ligand-reduced radical anion species, which were confirmed by

electrospectrochemistry and ESR measurements after electrolysis. The ligand-reduced species could react with alkyl halides to afford Co(III)-alkyl complexes and their reduction potentials and reactivity could be controlled by the substituents at the *meso* positions. The Co(III)- CH_3 complexes **7**, **8** and **9** were synthesized and characterized by ¹H NMR and MS. Catalytic reactions using the cobalt porphycenes were also performed and the product ratio of the dimer and dechlorinated form of the substrate were found to be changed by the catalyst and reduction potential. The ligand reduction mechanism for the formation of the Co(III)-alkyl complex became more useful for easier synthesis of the cobalt porphycenes and it also enabled easier control of the reduction potential of the ligand.

Acknowledgments

This work was partially supported by JSPS KAKENHI Grant Number 18H04265 in Precisely Designed Catalysts with Customized Scaffolding, Grant Number JP16H04119 (Grant-in-Aid for Scientific Research for Y. H.), and Grant Number JP17H04875 (Grant-in-Aid for Young Scientists (A) for T. O.), and by JSPS and PAN under the Research Cooperative Program Grant Number AJ179063(29-9111-t11). T. K. is grateful for the financial support from the Toyota Physical and Chemical Research Institute, Tonen General Sekiyu, Casio Science Promotion Foundation and Kyushu University QR program.

Supporting information

Spectroelectrochemical measurements, ESR spectra, ¹H NMR spectra, cyclic voltammetry and UV-vis absorption spectra are given in the supplementary material. This material is available free of charge via the Internet at <http://www.worldscinet.com/jpp/jpp.shtml>. Crystallographic data have been deposited at the Cambridge Crystallographic Data Centre (CCDC) under numbers CCDC 1910791 (**5**). Copies can be obtained on request, free of charge, via http://www.ccdc.cam.ac.uk/data_request/cif or from the Cambridge Crystallographic Data Centre, 12 Union Road, Cambridge CB2 1EZ, UK (fax: +44 1223-336-033 or email: deposit@ccdc.cam.ac.uk).

REFERENCES

1. van der Vlugt JI. *Chem. — Eur. J.* 2019; **25**: 2651–2662.
2. Luca OR and Crabtree RH. *Chem. Soc. Rev.* 2013; **42**: 1440–1459.
3. Lyaskovskyy V and de Bruin B. *ACS Catal.* 2012; **2**: 270–279.
4. Shimakoshi H and Hisaeda Y. *Current Opinion in Electrochemistry* 2018; **8**: 24–30.

5. Tahara K, Pan L, Ono T and Hisaeda Y. *Beilstein J. Org. Chem.* 2018; **14**: 2553–2567.
6. Morita Y, Oohora K, Sawada A, Kamachi T, Yoshizawa K and Hayashi T. *Inorg. Chem.* 2017; **56**: 1950–1955.
7. Giedyk M, Goliszewska K and Gryko D. *Chem. Soc. Rev.* 2015; **44**: 3391–3404.
8. Lexa D and Saveant J-M. *Acc. Chem. Res.* 1983; **16**: 235–243.
9. Wayland BB, Gridnev AA, Ittel SD and Frydlic M. *Inorg. Chem.* 1994; **33**: 3830–3833.
10. Ogoshi H, Watanabe E, Koketsu N and Yoshida Z. *Bull. Chem. Soc. Jpn.* 1976; **49**: 2529–2536.
11. Zheng GD, Yan Y, Gao S, Tong SL, Gao D and Zhen KJ. *Electrochim. Acta* 1996; **41**: 177–182.
12. Zhu W, Fang Y, Shen W, Lu G, Zhang Y, Ou Z and Kadish KM. *J. Porphyrins Phthalocyanines* 2011; **15**: 66–74.
13. Maiya GB, Han BC and Kadish KM. *Langmuir* 1989; **5**: 645–650.
14. Lexa D, Saveant J-M, Su K-B and Wang D-L. *J. Am. Chem. Soc.* 1988; **110**: 7617–7625.
15. Kadish KM, Lin XQ and Han BC. *Inorg. Chem.* 1987; **26**: 4161–4167.
16. Wayland BB, Gridnev AA, Ittel SD and Frydlic M. *Inorg. Chem.* 1994; **33**: 3830–3833.
17. Glod G, Angst W, Holliger C and Schwarzenbach R. *Environ. Sci. Technol.* 1997; **31**: 253–260.
18. Smith AL, Hardcastle KI and Soper JD. *J. Am. Chem. Soc.* 2010; **132**: 14358–14360.
19. Dzik WI, van der Vlugt JI, Reek JNH and de Bruin B. *Angew. Chem., Int. Ed.* 2011; **50**: 3356–3358.
20. Paul GC, Ghorai S and Mukherjee C. *Chem. Commun.* 2017; **53**: 8022–8025.
21. Bowman AC, Milsmann C, Atienza CCH, Lobkovsky E, Wieghardt K and Chirik PJ. *J. Am. Chem. Soc.* 2010; **132**: 1676–1684.
22. Semproni SP, Milsmann C and Chirik PJ. *J. Am. Chem. Soc.* 2014; **136**: 9211–9224.
23. Shiga T, Kumamaru R, Newton GN and Oshio H. *Dalton Trans.* 2018; **47**: 7804–7811.
24. Koide T, Aritome I, Saeki T, Morita Y, Shiota Y, Yoshizawa K, Shimakoshi H and Hisaeda Y. *ACS Omega* 2018; **3**: 4027–4034.
25. Gisselbrecht JP, Gross M, Köcher M, Lausmann M and Vogel E. *J. Am. Chem. Soc.* 1990; **112**: 8618–8620.
26. Bernard C, Gisselbrecht J, Gross M and Vogel E. *Inorg. Chem.* 1994; **33**: 2393–2401.
27. Kadish KM, Boulas PL, Kisters M, Vogel E, Aukauloo AM, D'Souza F and Guillard R. *Inorg. Chem.* 1998; **37**: 2693–2700.
28. Hashimoto K, Koide T, Okawara T, Shimakoshi H, Hori Y, Shiota Y, Yoshizawa K and Hisaeda Y. *Dalton Trans.* 2019; **48**: 872–881.
29. Sánchez-García D and Sessler JL. *Chem. Soc. Rev.* 2008; **37**: 215–232.
30. Anguera G and Sánchez-García D. *Chem. Rev.* 2017; **117**: 2481–2516.
31. Anju KS, Ramakrishnan S, Thomas AP, Suresh E and Srinivasan A. *Org. Lett.* 2008; **10**: 5545–5548.
32. Ganapathi E, Chatterjee T and Ravikanth M. *Eur. J. Org. Chem.* 2014; 6701–6706.
33. Ono T, Xu N, Koga D, Ideo T, Sugimoto M and Hisaeda Y. *RSC Adv.* 2018; **8**: 39269–39273.
34. Sakakibara E, Shisaka Y, Onoda H, Koga D, Xu N, Ono T, Hisaeda Y, Sugimoto H, Shiro Y, Watanabe Y and Shoji O. *RSC Adv.* 2019; **9**: 18697–18702.
35. Shimakoshi H, Luo Z, Inaba T and Hisaeda Y. *Dalton Trans.* 2016; **45**: 10173–10180.
36. Crystal data for **5** (from CH₂Cl₂/hexane): C₉₀H₄₄Cl₃Co₂F₁₆N₈, Fw 1765.54, monoclinic, space group P2₁/c, *a* = 8.7161 (4), *b* = 12.4531 (6), *c* = 18.1269 (8) Å, β = 99.414 (4), *V* = 1941.04 (16) Å³, *Z* = 1, *T* = 123 K, *d* = 1.51 g cm⁻³, GOF = 1.071, *R*₁ (*I* > 2σ(*I*)) = 0.0573 and *wR*₂ = 0.1780 (all data), CCDC 1910791.
37. The cobalt-methyl complexes **7–9** were unstable to light and heat and the corresponding mass peaks were not observed by ESI-TOF MS. In the observed absorption spectra of **7**, **8** and **9**, the absorption bands around 330 nm, which are characteristic to the Co(II) species, were weaker than those of **4**, **5**, and **6**, indicating the valence of the central cobalt was mainly +3 (Fig. S10) [38].
38. Hayashi T, Okazaki K, Shimakoshi H, Tani F, Naruta Y and Hisaeda Y. *Chem. Lett.* 2000; **2**: 90–91.